Accepted Manuscript

Design, synthesis and biological evaluation of novel pyridine-thiazolidinone derivatives as anticancer agents: Targeting human carbonic anhydrase IX

Fawad Ansari, Danish Idrees, Md Imtaiyaz Hassan, Kamal Ahmad, Fernando Avecilla, Amir Azam

PII: S0223-5234(17)31081-4

DOI: 10.1016/j.ejmech.2017.12.049

Reference: EJMECH 10027

To appear in: *European Journal of Medicinal Chemistry*

Received Date: 10 August 2017

Revised Date: 12 December 2017

Accepted Date: 13 December 2017

Please cite this article as: F. Ansari, D. Idrees, M.I. Hassan, K. Ahmad, F. Avecilla, A. Azam, Design, synthesis and biological evaluation of novel pyridine-thiazolidinone derivatives as anticancer agents: Targeting human carbonic anhydrase IX, *European Journal of Medicinal Chemistry* (2018), doi: 10.1016/j.ejmech.2017.12.049.

Design, synthesis and biological evaluation of novel pyridine-thiazolidinone derivatives as anticancer agents: Targeting human carbonic anhydrase IX

Fawad Ansari[1], Danish Idrees[2], Md. Imtaiyaz Hassan[2], Kamal Ahmad[2], Fernando Avecilla[3], Amir Azam[1,*]

[1]*Department of Chemistry, Jamia Millia Islamia, Jamia Nagar, 110 025, New Delhi, India*

[2]*Centre for Interdisciplinary Research in Basic Science, Jamia Nagar, 110 025, New Delhi, India*

[3]*Grupo Xenomar, Centro de Investigacións Científicas Avanzadas (CICA), Departamento de Química, Facultade de Ciencias, Universidade da Coruña, Campus de A Coruña, 15071 A Coruña, Spain**

Corresponding author. Tel.: +91 11 2698 1717/3253;

fax: +91 11 2698 0229/1232. E-mail address: amir_sumbul@yahoo.co.in (A. Azam)

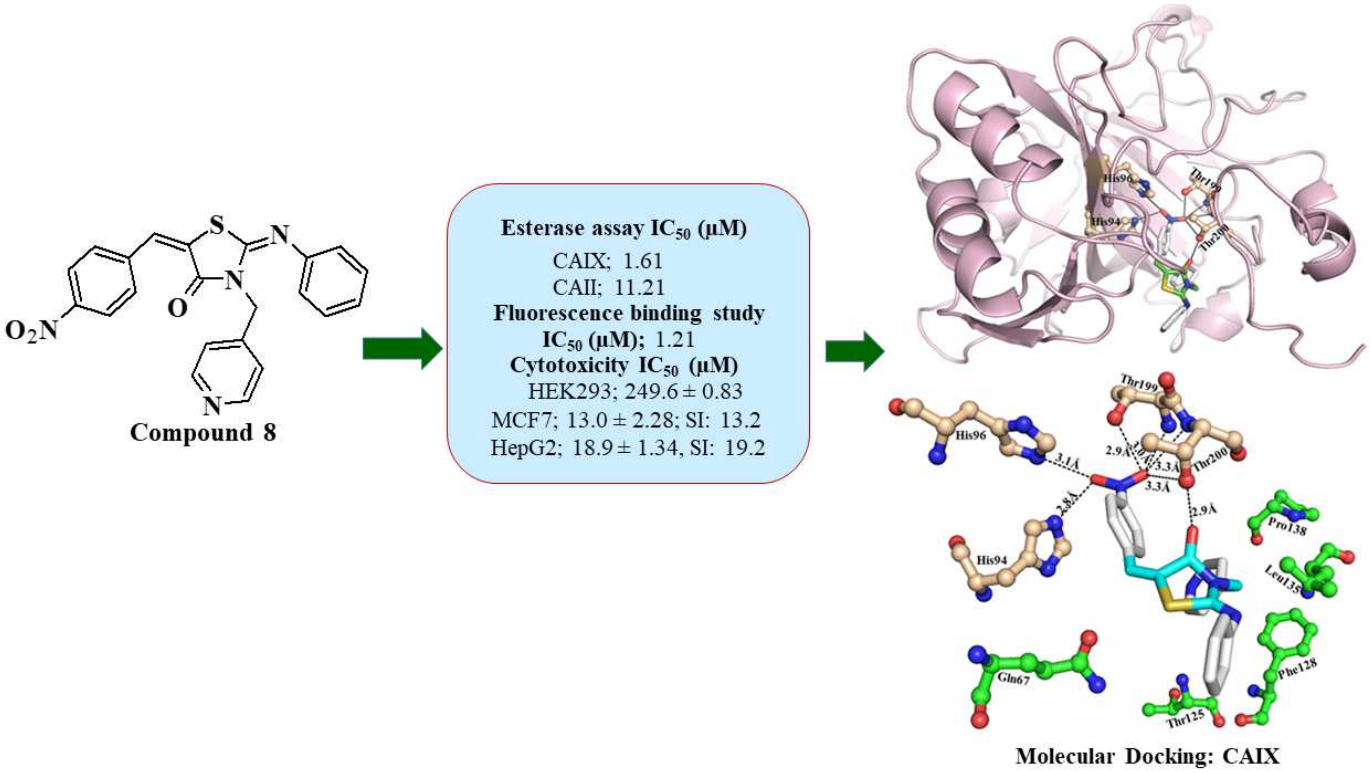

Design, synthesis and biological evaluation of novel pyridine-thiazolidinone derivatives as anticancer agents: Targeting human carbonic anhydrase IX

Mohammad Fawad Ansari[1], Danish Idrees[2], Md. Imtaiyaz Hassan[2], Kamal Ahmad[2], Fernando Avecilla[3], Amir Azam[1,*]

[1]*Department of Chemistry, Jamia Millia Islamia, Jamia Nagar, 110 025, New Delhi, India*
[2]*Centre for Interdisciplinary Research in Basic Science, Jamia Nagar, 110 025, New Delhi, India*
[3]*Grupo Xenomar, Centro de Investigacións Científicas Avanzadas (CICA), Departamento de Química, Facultade de Ciencias, Universidade da Coruña, Campus de A Coruña, 15071 A Coruña, Spain*

*To whom correspondence should be addressed: tel.: +91 11 2698 1717/3254; fax: +91 11 26980229; E-mail: amir_sumbul@yahoo.co.in

Abstract

In order to obtain novel Human carbonic anhydrase IX (CAIX) inhibitors, a series of pyridine-thiazolidinone derivatives was synthesised and characterized by various spectroscopic techniques. The binding affinity of the compounds was measured by fluorescence binding studies and enzyme inhibition activity using esterase assay of CAIX. It was observed that compound **8** and **11** significantly inhibit the CAIX activity with the IC_{50} value, 1.61 µM and 1.84 µM, respectively. The binding-affinity of compound **8** and **11** for CAIX was significantly high with their K_D values 11.21 µM and 2.32 µM, respectively. Docking studies revealed that compound **8** and **11** efficiently binds in the active site cavity of CA IX by forming sufficient numbers of H-bonds and van der Waals interactions with active side residues. All the compounds were further screened *in vitro* for anticancer activity and found that compound **8** and **11** exhibit considerable anticancer activity against MCF-7 and HepG-2 cell lines. All these findings suggest that compound **8** and **11** may be further exploited as a novel pharmacophore model for the development of anticancer agents.

***Key words*:** Pyridine, Thiazolidinone, Anticancer activity, Carbonic anhydrase.

1. Introduction

Cancer is considered as the second major cause of the death after cardiovascular disorders worldwide [1]. The inability to to distinguish between normal cell and cancerous cell has been the main drawback of the present chemotherapeutic system [2]. In past two decades, studies based on screening of the compounds for inhibition of tumour growth have been shifted towards the identification of novel therapeutic targets [3]. Therefore, development of safe and effective chemotherapeutic agents has been the major challenge to the medicinal chemists.

Currently, in the field of medicinal chemistry, five membered heterocyclic compounds received the special concern, especially compounds having two hetero atom showed a diverse range of biological activities [4-13]. Thiazolidinone is considered as indispensable anchor for development of new therapeutic agents because this five membered magic moiety possesses all types of biological activities [14-20]. The successful introduction of ralitoline as a potent anticonvulsant, etozoline as an antihypertensive, pioglitazone as a hypoglycemic agent and thiazolidomycin as antifungal agent proved the diverse range of biological activities associated with thiazolidinone moiety (**Figure 1**) [21].

A variety of thiazolidinone based derivatives having different substituents around the core nucleus are being considered as potential anticancer agents (**Figure 2**) [22-30]. Antitumor activity of these compounds may be due to their affinity toward various biological targets, such as JNK-stimulating phosphatase-1 (JSP-1) [31], phosphatase of a regenerating liver (PRL-3) [32-33], non-membrane protein tyrosine phosphatase (SHP-2) [34], tumour necrosis factor TNFα [35], antiapoptotic biocomplex Bcl-XL-BH3 [36], integrin avb3 [37], etc.

Furthermore, pyridine nucleus a well-studied six-membered heterocyclic moiety also displayed various biological activities, and is found in a variety of drugs such as isoniazid, ethionamide, amrinone, bupicomide, sulphapyridine, etc. [38]. It is reported in the literature that molecular hybridization of two or more biologically active pharmacophore into a single chemical structure showed significant synergistic effects [39]. The combination of thiazolidinones with other heterocyclic rings showed wide range of biological activities [40].

Recently, thiazolo- linked pyrimidine and thiazolidinone-oxoindoline base compounds have been used as a potent CA inhibitor [41-42]. Hence, thiazolidinone coupled pyridine molecules would be a promising scaffold for the development of potent CAIX inhibitors toward the anticancer therapy. CAIX is an attractive target for cancer treatment because of its limited expression in the normal tissues and predominant expression in varieties of tumour cells [43]. CAIX is a hypoxia-inducible protein that regulates cellular pH to encourage cancer cell survival [44]. Moreover, it contributes to cancer progression by stimulating cancer cell migration, adhesion and invasion [45]. Nowadays CAIX has been identified as an important biomarker of hypoxia and its over-expression is often associated with a poor responsiveness to the classical radio and chemotherapies [46].

The present study reports the synthesis, characterization, CAIX inhibition activity of pyridine-thiazolidinone derivatives and their screening against breast and liver cancer cell lines along with normal cell line.

2. Results and Discussion

2.1. Chemistry

The synthetic route for the synthesis of the desired pyridine-thiazolidinone derivatives are shown in the **Scheme 1**. 1-Phenyl-3-(pyridine-4-ylmethyl)thiourea **1** were synthesized by reacting isothiocyanate with 4-picolylamine in toluene. 1-Phenyl-3-(pyridine-4-ylmethyl)thiourea **1** in presence of anhydrous sodium acetate and monochloroacetic acid undergo cyclization to form 2(phenylimino)-3-(pyridine-4-ylmethyl)thiazolidin-4-one **2**, which on further reaction with different aldehyde derivatives in presence of piperidine, ethanol as solvent gave the final products **3-20**. The structure of synthesised compounds was confirmed by IR, ^{1}H NMR, ^{13}C NMR and mass spectrometry. Elemental analysis justified the purity of the compounds.

2.1.1. Single crystal structure

2.1.2. Single crystal structures of 2, 3, 6 and 12

The compounds crystallize in centrosymmetric space groups, **2** in a triclinic system, **3**, **6** and **12** in monoclinic system (**Table 1**). The asymmetric unit only contain one molecule of thiazolidin-4-one derivatives in all cases. The different benzyl groups bonded to C(1) are almost flat with thiazolindin-4-one group [C(1), C(2), C(3), S(1), N(1), C(16), C(17), C(18), C(19), C(20), C(21), C(22), mean deviation from plane, 0.0927(10) Å in **3**, 0.1358(10) Å in **6** and 0.1488(10) Å in **12**, which form dihedral angles with the phenyl groups of 76.18(3)º in **2**, 65.62(3)º in **3**, 57.61(3)º in **6** and 62.57(3)º in **12** and with the pyridine groups of 45.95(3)º in **2**, 61.52(4)º in **3**, 74.38(4)º in **6** and 59.42(5)º in **12 (Figure 3-6)**. (Bond lengths and angles are summarized in **Table SI 1 Supplementary data)**.

X-ray structure analysis of **2**, **3**, **6** and **12** shows two enantiomers of the compounds in the racemic crystals, the chirality being due to a twist of the phenyl and pyridine units. This enantiomerization occurs by simultaneously rotating about the two single bonds, N(1)-C(10) and

N(2)-C(4). The compounds present a mirror plane which contains the point of inversion (**Figures 7-10**) [47].

Depending on the substituents in the thiazolidinone rings, crystal structures adopt different crystal packing (**Figure 11**). The crystal packing of the structures don´t present π-π stacking interactions between the rings either hydrogen bonds as occur in other structures which contain thiazolindinone rings with other substituents [48].

2.2. Esterase assay

The inhibition activity of all synthesized compounds **1-20** was tested against human CAIX and CAII using the esterase activity, with 4-nitrophenyl acetate (4-NPA) as substrate. The inhibition data of target compounds are shown in **Table 2**. The inhibitor acetazolamide (AZM) was used as a standard to investigate the inhibitory activity of these compounds.

2.2.1. Structure Activity Relationship

Structure-activity relationship of pyridine-thiazolidinone derivatives **1-20** demonstrated that compounds having unsubstituted phenyl ring **3** and alkyl group substitution on phenyl ring; **4** and **10** showed less inhibitory activity against CAIX having IC_{50} = 50.92 µM, 57.31 µM and 63.11 µM respectively. Alkoxy substituted compounds; **6, 13** and **14** also showed less activity against CAIX with IC_{50} = 40.41 µM, 60.92 µM and 38.40 µM respectively. Compound **12** and **15** having disubstituted methoxy group displayed good inhibitory activity against CAIX (IC_{50} = 20.92 µM and 16.68 µM). Compound with chloro substituted; **7** and **17** were found to show lesser activity against CA IX with IC_{50} = 40.18 µM and 43.52 µM respectively.

Compound with nitro substitution on benzene ring **8** showed excellent inhibitory activity against CAIX with IC_{50} = 1.61 µM. SAR revealed that the compouds with hydroxyl groups had

excellent impact on CAIX inhibition activity. Among the hydroxyl group containing compound **5**, **11** and **16**, compound **11** having di-hydroxyl group exhibited excellent inhibitory activity against CA IX (IC_{50} = 1.84 µM). Further it was found that compounds having heterocyclic substitution **18** (IC_{50} = 6.64 µM) and compound **19 (**IC_{50} = 10.04 µM**)** displayed good binding inhibition aginst CAIX. On the basis of SAR studies it can be concluded that the compounds containing polar moieties **8** and **11** on phenyl ring were favourable for excellent inhibitory activity against CAIX. In fact the inhibiton of CAIX by a paricular compound not depends only on the nature of substituents but entire molecular skeleton is responsible for its activity.

To check the selectivity of compounds **8** and **11** against CAIX, these two compounds were tested against human CAII using the esterase activity (**Table 2**). The compounds **8** and **11** have shown selectivity for CAIX over CAII approximately 9 times and 14 times respectively.

2.3. Fluorescence binding study

The fluorescence emission spectra CAIX with increasing concentrations of compounds **8** and **11** in Tris at 25 °C are shown in **Figure 12** and **13**. The emission maxima peak of CAIX at 341 nm (λ_{exc}=280 nm) is drastically reduced on increasing concentrations (1–100 µM) of compounds, indicating a significant binding. The values fluorescence intensity at 341 nm was plotted as a function of [ligand] to calculate the binding affinity of compounds against CAIX (**Table 2**). The binding affinity of compound **8** for CAIX is 11.21 µM (**Figure 12**) and for compound **11** is 2.32 µM (**Figure 13**). Results clearly indicate that compounds **8** and **11** exhibited excellent affinity for CAIX.

2.4. Cytotoxicity assay

The cytotoxicity and cell proliferation activity of synthesized compounds **1-20** were evaluated by MTT assay. Human embryonic kidney normal cell line (HEK-293) was used for the cytotoxicity. Compounds **2, 5, 8, 10, 11, 12, 16, 18** and **19** were less toxic upto 100 µM on HEK-293 cells. The IC_{50} values of these compounds ranging from 99.5 µM to 249.6 µM as compared to standard drug doxorubicin 148.4 µM (**Table 2**).

The anticancer activity of these compounds against MCF-7 and HepG-2 with dose dependent concentration were studied and found cells viability reduced significantly, doxorubicin taken as standard in the experiment. In case of breast cancer cell line (MCF-7), compounds **5**, **8** and **11** showed good activity with IC_{50} value 18.9±2.19 µM, 13.0±2.28 µM and 12.4±1.39 µM while compounds **18** and **19** were moderately active with IC_{50} value 21.1±2.68 µM and 28.7±1.90 µM, respectively. Compound **9**, **10** and **12** having IC_{50} value 76.3±1.56 µM, 53.3±2.05 µM and 80.7±1.96 µM showed week activity against this cancer cell line.

Concerning activity against HepG-2, the synthesized pyridine-thiazolidinone hybrid showed good to moderate growth inhibitory activity. Compounds **5**, **8**, **11** and **16** were the most potent against HepG-2 as their IC_{50} values were 11.8±1.95 µM, 18.9±1.34 µM, 16.2±1.34 µM and 17.6±2.12 µM. Compounds **10**, **12**, **18** and **19** having IC_{50} value in the range of 23.1±1.90 µM - 32.3±1.48 µM were the moderately active against this cell line. Furthermore, compounds **9** and **15** showed fair antiproliferative activity with IC_{50} value 52.6±1.45 µM and 35.8±1.45 µM.

Selective index (SI) values were calculated for the effectiveness of synthesized compounds **1-20** against cancerous cells. High SI value (>3) of compounds gives a selective inhibition towards cancer cells. While the compounds with SI value <3 is considered to be toxic for normal cells [49]. Compounds **2**, **5**, **8**, **10**, **11**, **12**, **16**, **18** and **19** showed good selectivity against MCF-7, HepG-2 cell lines with the SI values more than 3 (**Table 2**). Interestingly, if we

compared and correlate the binding affinity and esterase activity of compounds with that of cytotoxicity activity, it was found that compound **8** and **11** which shows significant binding with CAIX, also inhibited the enzyme activity to the most. Consistant to the binding and activity results, these two compounds **8** and **11** also inhibited the cell viability of cancerous cells more pronouncly than other compounds. All these observations clearly suggested that the results of binding, enzyme activity and cell cytotoxicity are in good agreement with each other.

2.5. Molecular docking

Auto dock 4.2 was used to determine the orientation of inhibitors bound in the active site of the CAIX and the conformation with the highest binding energy value for each molecule was chosen for further analysis and results of these studies are given in **Table 3.** The binding mode of CAIX inhibitors are visualized by PyMOL [50]. The binding site CAIX has been used to elucidate the interactions as reported earlier [51].

The compounds **8** and **11** bind into the active site of CAIX with minimum binding energy (ΔG) −8.95 kcal/mol (K_i = 7.01µM) and −8.01 kcal/mol (K_i = 10.21µM), respectively as compared to AZM (ΔG) −6.43 kcal/mol (Ki = 14.04µM) [52] (**Table 3**). The nitrobenzylidine ring in compound **8** formed six H-bond interaction with His94, His96, Thr199 , Thr200 and one H-bond formed between thiazolidin-4-one and Thr200 (**Figure 14A**). Active site residues Gln67, Thr125, Phe128, Leu135 and Pro138 are involved in hydrophobic interaction and Tyr7 and Trp97 are stabilized phenylimino and nitrobenzylidine ring respectively of compound **8** with π–π interaction (**Figure 14B**).

At the active site of CAIX, compound **11** shows 7 H-bond interaction with Asn62, Gln92, Thr199, Thr199, whereas residues His64, Gln67, His119 and Val121 are involved in

hydrophobic interaction (**Figure 14C** and **D**). The 3, 4-dihydroxybenzylidine of compound **11** is stabilized with π–π interaction of His96. However, molecular docking result shows a quite different orientation of compounds **8** and **11** at the active site of CAIX due to substituent changing at 5 position of thiazolidin-4-one. These results supports our binding and enzyme activity results, that these compound **8** and **11** offers sufficient number of interactions to CAIX, resultantly formed a stable complex. Thus these results are also in close agreement with the results of binding, enzyme activity and cell viability studies.

3. Conclusion

A series of pyridine-thiazolidinone derivatives was synthesized and evaluated for their anticancer activity. CAIX inhibition and fluorescence binding studies have shown that compounds **8** and **11** were most effective inhibitors with a significant binding affinity and exhibits the highest selectivity towards MCF-7 and HepG-2 cell lines. Molecular docking studies showed that compounds **8** and **11** strongly bind to the active site residues of CAIX. In summary, compounds **8** and **11** potentially inhibits CAIX and may be further exploited to fight hypoxia-induced tumours in future studies.

4. Experimental

All chemicals were purchased from Merck and Aldrich Chemical Company (USA). Precoated aluminum sheets (Silica gel 60 F254, Merck Germany) were used for thin-layer chromatography (TLC) and spots were visualized under UV light. The melting points were recorded on Veego instrument with model specifications REC-22038 A2 and are uncorrected. Elemental analyses were performed on Elementar Vario analyzer and the results are within ±0.4% of the theoretical values. IR spectra were acquired at Bruker FT-IR spectrophotometer. ^{1}H

and ^{13}C NMR were recorded on a Bruker Spectrospin DPX 300 MHz and Bruker Spectrospin DPX 75 MHz spectrometer, respectively using $CDCl_3$ and DMSO-d_6 as a solvent and trimethylsilane (TMS) as the internal standard. Splitting patterns are designated as follows; s, singlet; d, doublet; t, triplet; m, multiplet. Chemical shift values are given in ppm. Mass spectra were recorded by ESI-MS (AB-Sciex 2000, Applied Biosystem).

4.1. Chemistry

4.1.1. General procedure for the synthesis of 1-phenyl-3-(pyridine-4-ylmethyl)thiourea (1)

On treating phenylisothiocyanate (59.17 mmol, 8g) with 4-picolinylamine (59.17 mmol, 6.39g) in toluene white precipitates were obtained which were collected by filtration, washed with toluene, and dried to afford 1-phenyl-3-(pyridine-4-ylmethyl)thiourea (**1)**.

4.1.1.1. 1-Phenyl-3-(pyridine-4-ylmethyl)thiourea (1) Yield: 90%; m.p.: 168˚C; Anal. Calc. (%) for $C_{13}H_{13}N_3S$: C 64.17, H 5.39, N 17.27, S 13.18; found: C 64.12, H 5.19, N 17.47, S 13.42; FT-IR ν_{max} (cm^{-1}): 3260 (NH), 3098 (C-H, Ar-H), 1235 (C=S); ^1H NMR ($CDCl_3$) δ (ppm): 4.92 (d, 2H, *J*=5.7 Hz, CH_2), 6.39 (s, 1H, N-H), 7.18-7.30 (m, 4H, Ar-H), 7.35 (d, 1H, *J*=6.9 Hz, Ar-H), 7.47 (t, 2H, *J*=7.2 Hz, Ar-H), 8.16 (s, 1H, N-H), 8.54 (d, 2H, *J*=7.5 Hz, Ar-H); ^{13}C NMR ($CDCl_3$) δ (ppm): 47.89, 76.59, 77.02, 77.44, 122.08, 125.64, 127.88, 130.42, 135.74, 146.65, 150.06, 181.88; ESI-MS: m/z = 244.0 (M^++1).

4.1.2. General procedure of synthesis of 2(phenylimino)-3-(pyridine-4-ylmethyl)thiazolidin-4-one (2)

1-phenyl-3-(pyridine-4-ylmethyl)thiourea (53.42 mmol, 13.0g) was dissolved in ethanol and then anhydrous sodium acetate (107.28 mmol, 8.8g) and chloroacetic acid (66.98 mmol, 6.33g) were added in the reaction mixture. The suspension was heated under reflux for 12 h and then the

solvent was evaporated. Water was added and the aqueous layer was extracted with ethyl acetate. The organic layer was washed with saturated sodium bicarbonate and brine. The combined organic extracts were dried over Na_2SO_4 and concentrated *in vacuo,* consequently yellow solid product 2(phenylimino)-3-(pyridine-4-ylmethyl)thiazolidin-4-one **2** was obtained.

4.1.2.1. 2-(Phenylimino)-3-(pyridine-4-ylmethyl)thiazolidin-4-one (2) Yield: 87%; m.p.: 122˚C; Anal. Calc. (%) for $C_{15}H_{13}N_3OS$: C 63.58, H 4.62, N 14.83, S 11.32; found: C 63.38, H 4.69, N 14.65, S 11.58; FT-IR ν_{max} (cm^{-1}): 1719 (-N-C=O), 1640 (C=N), 809 (C-S-C), 1371 (tert. N); ^1H NMR ($CDCl_3$) δ (ppm): 3.87 (s, 2H, S-CH_2-C=O), 5.02 (s, 2H, CH_2), 6.93 (d, 2H, *J*=7.5 Hz, Ar-H), 7.17 (t, 1H, *J*=7.2 Hz, Ar-H), 7.36 (t, 4H, *J*=6.0 Hz, Ar-H), 8.59 (d, 2H, *J*=5.7 Hz, Ar-H); ^{13}C NMR ($CDCl_3$) δ (ppm): 32.69, 45.16, 76.61, 77.04, 77.46, 120.87, 123.30, 124.87, 129.31, 144.38, 147.47, 150.10, 153.47, 171.42; ESI-MS: m/z = 284.1 (M^++1).

4.1.3. General procedure of synthesis of 2(phenylimino)-3-(pyridine-4-ylmethyl)thiazolidin-4-one hybrids (3-20)

A mixture of 3-(furan-2-ylmethyl)-2-(phenylimino)-1, 3-thiazolidin-4-one (2.00 mmol, 0.56g), different aldehydes (2.00 mmol, 0.21-.33g), hexahydropyridine (2.30 mmol, 0.19g), and ethanol (35 mL) were heated under reflux for 11-12 h. The reaction mixture was cooled to room temperature and the precipitates were obtained which were filtered, washed and recrystallized from ethanol to furnished final products **3-20**.

4.1.3.1. 5-Benzylidene-2-phenylimino-3-pyridine-4-ylmethyl-thiazolidin-4-one (3) Yield: 84%; m.p.: 162˚C; Anal. Calc. (%) for $C_{22}H_{17}N_3OS$: C 71.14, H 4.61, N 11.31, S 8.63; found: C 71.38, H 4.33, N 11.10, S 8.31; FT-IR ν_{max} (cm^{-1}): 1706 (-N-C=O), 1640 (C=N), 760 (C-S-C), 1375 (tert. N), 1583 (C=C); ^1H NMR ($CDCl_3$) δ (ppm): 5.17 (s, 2H, CH_2), 6.98 (d, 2H, *J*=7.5 Hz, Ar-

H), 7.22 (d, 2H, *J*=7.2 Hz, Ar-H), 7.38-7.43 (m, 8H, Ar-H), 7.79 (s, 1H, CH=C), 8.60 (s, 2H, Ar-H); ^{13}C NMR ($CDCl_3$) δ (ppm): 45.19, 121.07, 123.21, 125.11, 129.08, 129.44, 130.02, 130.08, 131.77, 133.53, 140.11, 144.53, 147.66, 149.71, 150.14, 166.52; ESI-MS: m/z = 372.1 (M^++1).

4.1.3.2. 5-(4-Methylbenzylidene)-2-(phenylimino)-3-(pyridine-4-ylmethyl)thiazolidin-4-one (4)

Yield: 82%; m.p.: 165˚C; Anal. Calc. (%) for $C_{23}H_{19}N_3OS$: C 71.66, H 4.97, N 10.90, S 8.32; found: C 71.91, H 4.61, N 11.15, S 8.21; FT-IR ν_{max} (cm^{-1}): 1703 (-N-C=O), 1653 (C=N), 764 (C-S-C), 1381 (tert. N), 1578 (C=C); ^{1}H NMR ($CDCl_3$) δ (ppm): 2.36 (s, 3H, CH_3), 5.16 (s, 2H, CH_2), 6.98 (d, 2H, *J*=7.5 Hz, Ar-H), 7.22 (d, 1H, *J*=7.5 Hz, Ar-H), 7.33-7.39 (m, 6H, Ar-H), 7.77 (s, 1H, CH=C), 8.59 (d, 2H, *J*=4.5 Hz, Ar-H); ^{13}C NMR ($CDCl_3$) δ (ppm): 21.25, 45.14, 76.64, 77.06, 77.49, 119.85, 121.10, 123.20, 125.04, 129.41, 129.83, 130.08, 130.79, 131.89, 140.67, 144.62, 147.74, 149.87, 150.12, 166.62; ESI-MS: m/z = 386.1 (M^++1).

4.2. Crystal structure determination

X-ray data were collected on a Bruker Kappa Apex CCD diffractometer at low temperature for **2**, **3**, **6** and **12**, by the ϕ-ω scan method. Reflections were measured from a hemisphere of data collected from frames, each of them covering 0.3º in ω. A total of 40101 for **2**, 47051 for **3**, 55044 for **6**, and 69246 for **12**, reflections measured were corrected for Lorentz and polarization effects and for absorption by multi-scan methods based on symmetry-equivalent and repeated reflections. Of the total, 3876 for **2**, 4193 for **3**, 4374 for **6** and 5584 for **12**, independent reflections exceeded the significance level ($|F|/\sigma|F|$) > 4.0. After data collection, in each case a multi-scan absorption correction (SADABS) [53] was applied, and the structure was solved by direct methods and refined by full matrix least-squares on F^2 data using SHELX suite of programs [54]. Hydrogen atoms were located in difference Fourier map and left to refine

freely. Refinements were done with allowance for thermal anisotropy of all non-hydrogen atoms. A final difference Fourier map showed no residual density outside: 0.503 and -0.205 e.Å^{-3} for **2**, 0.346 and -0.293 for **3** e.Å^{-3}, 0.344 and -0.279 e.Å^{-3} for **6** and 0.469 and -0.425 e.Å^{-3} for **12**. A weighting scheme w = 1/[$\sigma^2(F_o^2)$ + (0.040400 P)^2 + 0.296300 P] for **2**, w = 1/[$\sigma^2(F_o^2)$ + (0.041100 P)^2 + 0.905000 P] for **3,** w = 1/[$\sigma^2(F_o^2)$ + (0.054100 P)^2 + 2.207800 P] for **6** and w = 1/[$\sigma^2(F_o^2)$ + (0.063300 P)^2 + 0.570100 P] for **12**, where P = ($|F_o|^2$ + 2$|F_c|^2$)/3, were used in the latter stages of refinement. Further details of the crystal structure determination are given in **Table 1.** CCDC 1564721-1564724 contain the supplementary crystallographic data for the structures reported in this paper. These data can be obtained free of charge via http://www.ccdc.cam.ac.uk/conts/retrieving.html, or from the Cambridge Crystallographic Data Centre, 12 Union Road, Cambridge CB2 1EZ, UK; fax: (+44) 1223 336 033; or e-mail: deposit@ccdc.cam.ac.uk. Supplementary data associated with this article can be found, in the online version, at doi: $$$$$.

4.3. Biological Evaluation

4.3.1. Esterase assay

CAs inhibition was measured by following the change in absorbance at 400 nm of p-nitrophenyl acetate (4-NPA) to p-nitrophenol (a yellow colour compound). This method is based on spectrophotometric determination of p-nitrophenol which is formed as CA catalysed hydrolysis 4-NPA. Esterase assay was performed in buffer containing 50 mM Tris pH 8.0, 100 mM NaCl, and 1mM EDTA. Acetazolamide (AZM) and test compounds (**1-20**) were in 100% DMSO. The concentration of CAIX was used 1 µM and 4-NPA was used in 0.5 mM concentration. Test compounds concentration was used in 0.01 to 100 µM in a final volume of 100µl. Stock solutions and dilutions of inhibitors were prepared in DMSO such that there was a

constant 1% DMSO in the assay. The reaction was initiated by addition of 4-NPA and reading was taken after 3 min incubation of test compounds at 25 °C. The absorbance of each well was measured with a Spectra Max Plus384 microplate spectrophotometer (Molecular Devices, Sunnyvale, CA). IC_{50} values for each test compounds were calculated by using Graph Pad Prism (Version 5.0) graphing software.

4.3.2. Fluorescence Measurements

Fluorescence measurements were performed on Jasco-spectrofluorimeter (Model FP-6200) using 5 mm quartz cuvette. The protein concentration 0.5 μM was used for CAIX. Working solutions of compounds were made in 50mM Tris buffer, pH 8.0. and used in the concentration 1-100 μM. Protein was excited at 280 nm and the emission spectra were recorded between 300 - 400 nm at 25 °C using slits with a 5 nm band pass for excitation and emission, respectively. Final spectrum was collected after subtracting intensity of the buffer from each sample spectrum. Fluorescence-quenching studies were carried out and the results have also been used to estimate the binding affinity by Stern–Volmer equations with slight modification.

$$\log(F_o - F)/F = \log Ka + n\log[Q] \qquad (1)$$

Where F_o is the fluorescence intensity of protein and F is the fluorescence intensity of ligand, *K*a is the binding constant and n is the number of binding sites, Q represents quenching constant. For the ligand–protein complex, the values for Ka and n can be derived from the intercept and slope.

4.3.3. Cell Culture

Human breast cancer cells (MCF-7), human liver cancer cells (HepG-2) and human embryonic kidney cells (HEK-293) were obtained from National Centre for Cell Science, Pune, India. The cells were cultured in Roswell Park Memorial Institute (RPMI) (Sigma Aldrich) with

10% foetal bovine serum (Gibco-life technologies), 1% penicillin-streptomycin-Neomycin in a humidified 5% CO_2 atmosphere at 37 $^{\circ}$C. Cells were routinely cultured and maintained not more than 35 passages.

4.3.4. Cytotoxicity assay

The cell cytotoxicity was detected by standard MTT (3-(4,5-dimethylthiazol-2-yl)-2,5-diphenyl tetrazolium bromide) assay [55-56]. Approximately, 5×10^3 cells/well were seeded into the 96-well plate media containing fetal bovine serum (10%) and 1 % penicillin–streptomycin and then incubated in a humidified 5 % CO_2 atmosphere at 37 $^{\circ}$C overnight. After 24 h incubation, media were removed, and reduce serum media were added for serum starvation. The next day, media were replaced with 200 µL of fresh complete medium containing different concentrations of compounds and doxorubicin ranging from 2.5 µM to 80 µM for cancer cell lines and from 5 µM to 200 µM for HEK 293. Doxorubicin was included as standard reference drug (positive control). After 48 h, the supernatants were removed, and cell were washed with PBS and 20 µL of MTT solution (5 mg/mL in PBS) was added to each well, and the cells were incubated at 37 $^{\circ}$C in a humidified chamber for 4 h. After 4 h, the supernatant was removed from each well and the coloured formazan crystal produced from MTT was dissolved in 100 µL of DMSO. The absorbance was measured at 570 nm by using enzyme linked immune absorbent assay reader (BioRad). The IC_{50} values of the tested compound were estimated using the best fit regression curve method in Excel. All experiments were repeated at least three times.

4.3.5. Calculation of the selectivity index

The selectivity index corresponded to the IC_{50} value determined for activity of synthesized compounds and reference compound on HEK-293 cells divided by the IC_{50}

determined for cancer cells (MCF-7 and HepG-2). The selectivity index values greater than three was considered significant [55, 57].

4.3.6. Preparation of Ligands and Protein Molecule

The structures of ligands were drawn by using the software ChemBioDraw Office 12.0 (licensed @ Cambridge's soft). The PDB file of ligand was then generated and converted into PDBQT file by process like detect root, chose the torsion and set the number of torsion by using ADT [58]. Crystal structure of CAIX was taken from the Protein Data Bank (www.rcsb.org) [59]. Then, the hydrogen atoms having polar nature were added, the residue structures having lower occupancy were deleted, and the side chains that were incomplete were then replaced by using Auto Dock Tools (ADT) version 1.5.6 from the Scripps Research Institute. Further, to each atom having Gasteiger charges were added and the non-polar hydrogen atoms were merged to the protein structure. After that the structures constructed were saved in PDBQT file format, for further analysis in ADT [59].

4.3.7. Molecular docking

Molecular docking stimulation using the ligand molecules with CAIX (PDB ID: 3IAI) was conducted using Autodock 4.2 docking suite by employing Lamarckian genetic algorithm [60]. The ligands were set to explore and flexible to rotate most probable binding poses, while receptor was kept rigid. The grid maps representing the center of active site pocket for the ligand were calculated with Autogrid. The dimensions of the grid for CAIX was 85 × 85 × 85 grid points with a spacing of 0.435 Å between the grid points but center on the ligand for receptor (64.496, 61.661 and -8.547 coordinates). In the present docking study was performed by each run with population of 150 individuals, rate of gene mutation 0.02, cross-over rate 0.8 and the

remaining parameters were set as default [51, 53]. Ten poses docking conformations were generated and the best docked conformation was selected based on the Autodock binding energy (Kcal/mol), for further analysis. Finally, the conformations with the most favourable free binding energy were selected for analyzing the interactions between the target receptor and ligands by PyMOL [61-62].

Acknowledgement

One of the authors MFA is thankful to University Grant Commission, India for providing BSR meritorious fellowship.

References

[1] Jemal, A., Bray, F., Center, M.M., Ferlay, J., Ward, E. and Forman, D., 2011. Global cancer statistics. *CA Cancer J. Clin.*, 61, 69-90.

[2] Zwick, E., Bange, J. and Ullrich, A., 2001. Receptor tyrosine kinase signalling as a target for cancer intervention strategies. *Endocr. Relat. Cancer*, 8, 161-173.

[3] Grever, M.R., Schepartz, S.A. and Chabner, B.A., 1992, December. The National Cancer Institute: cancer drug discovery and development program. In *Seminars in oncology* (Vol. 19, No. 6, 622-638). Independence Square West Curtis Center, STE 300, Philadelphia, PA 19106-3399: WB Saunders CO.

[4] Romagnoli, R., Baraldi, P.G., Prencipe, F., Oliva, P., Baraldi, S., Salvador, M.K., Lopez-Cara, L.C., Brancale, A., Ferla, S., Hamel, E. and Ronca, R., 2017. Synthesis and Biological Evaluation of 2-Methyl-4, 5-Disubstituted Oxazoles as a Novel Class of Highly Potent Antitubulin Agents. *Sci. Rep.*, 7.

[5] Dewangan, D., Kumar, T., Alexander, A., Nagori, K. and Tripathi, D.K., 2011. Pyrazole: Their Chemistry and Pharmacological Potentials: A Review. *Curr Pharma Res*, 1, 369.

[6] Li, Y.S., Hu, D.K., Zhao, D.S., Liu, X.Y., Jin, H.W., Song, G.P., Cui, Z.N. and Zhang, L.H., 2017. Design, synthesis and biological evaluation of 2, 4-disubstituted oxazole derivatives as potential PDE4 inhibitors. *Bioorg. Med. Chem.*, 25, 1852-1859.

[7] Ansari, M.F., Siddiqui, S.M., Agarwal, S.M., Vikramdeo, K.S., Mondal, N. and Azam, A., 2015. Metronidazole hydrazone conjugates: design, synthesis, antiamoebic and molecular docking studies. *Bioorg. Med. Chem. Lett.*, 25, 3545-3549.

[8] Jin, R.Y., Sun, X.H., Liu, Y.F., Long, W., Chen, B., Shen, S.Q. and Ma, H.X., 2016. Synthesis, crystal structure, biological activity and theoretical calculations of novel isoxazole derivatives. *Spectrochim. Acta A Mol. Biomol. Spectrosc.*, 152, 226-232.

[9] Tomi, I.H., Tomma, J.H., Al-Daraji, A.H. and Al-Dujaili, A.H., 2015. Synthesis, characterization and comparative study the microbial activity of some heterocyclic compounds containing oxazole and benzothiazole moieties. *J.Saudi Chem. Soc.*, 19, 392-398.

[10] Rouf, A. and Tanyeli, C., 2015. Bioactive thiazole and benzothiazole derivatives. *Eur. J. Med. Chem.*, 97, 911-927.

[11] Su, Q., Ioannidis, S., Chuaqui, C., Almeida, L., Alimzhanov, M., Bebernitz, G., Bell, K., Block, M., Howard, T., Huang, S. and Huszar, D., 2013. Discovery of 1-Methyl-1 H-imidazole Derivatives as Potent Jak2 Inhibitors. *J. Med. Chem.*, 57, 144-158.

[12] Lan, R., Liu, Q., Fan, P., Lin, S., Fernando, S.R., McCallion, D., Pertwee, R. and Makriyannis, A., 1999. Structure-activity relationships of pyrazole derivatives as cannabinoid receptor antagonists. *J. Med. Chem.*, 42, 769-776.

[13] Nakamura, T., Sato, M., Kakinuma, H., Miyata, N., Taniguchi, K., Bando, K., Koda, A. and Kameo, K., 2003. Pyrazole and isoxazole derivatives as new, potent, and selective 20-hydroxy-5, 8, 11, 14-eicosatetraenoic acid synthase inhibitors. *J. Med. Chem.*, 46, 5416-5427.

[14] Patel, N.B. and Shaikh, F.M., 2010. Synthesis and antimicrobial activity of new 4-thiazolidinone derivatives containing 2-amino-6-methoxybenzothiazole. *Saudi Pharm. J.*, 18, 129-136.

[15] Hu, J., Wang, Y., Wei, X., Wu, X., Chen, G., Cao, G., Shen, X., Zhang, X., Tang, Q., Liang, G. and Li, X., 2013. Synthesis and biological evaluation of novel thiazolidinone derivatives as potential anti-inflammatory agents. *Eur. J. Med. Chem.*, 64, 292-301.

[16] Omar, K., Geronikaki, A., Zoumpoulakis, P., Camoutsis, C., Soković, M., Ćirić, A. and Glamočlija, J., 2010. Novel 4-thiazolidinone derivatives as potential antifungal and antibacterial drugs. *Bioorg. Med. Chem.*, 18, 426-432.

[17] Ruiz, F.A.R., García-Sánchez, R.N., Estupiñan, S.V., Gómez-Barrio, A., Amado, D.F.T., Pérez-Solórzano, B.M., Nogal-Ruiz, J.J., Martínez-Fernández, A.R. and Kouznetsov, V.V., 2011. Synthesis and antimalarial activity of new heterocyclic hybrids based on chloroquine and thiazolidinone scaffolds. *Bioorg. Med. Chem.*, 19, 4562-4573.

[18] Shiradkar, M.R., Ghodake, M., Bothara, K.G., Bhandari, S.V., Nikalje, A., Akula, K.C., Desai, N.C. and Burange, P.J., 2007. Synthesis and anticonvulsant activity of clubbed thiazolidinone–barbituric acid and thiazolidinone–triazole derivatives. *Arkivoc*, 14, 58-74.

[19] Ravichandran, V., Kumar, B.P., Sankar, S. and Agrawal, R.K., 2009. Predicting anti-HIV activity of 1, 3, 4-thiazolidinone derivatives: 3D-QSAR approach. *Eur. J. Med. Chem.*, 44, 1180-1187.

[20] Ottanà, R., Maccari, R., Giglio, M., Del Corso, A., Cappiello, M., Mura, U., Cosconati, S., Marinelli, L., Novellino, E., Sartini, S. and La Motta, C., 2011. Identification of 5-arylidene-4-thiazolidinone derivatives endowed with dual activity as aldose reductase inhibitors and antioxidant agents for the treatment of diabetic complications. *Eur. J. Med. Chem.*, 46, 2797-2806.

[21] Jain, A.K., Vaidya, A., Ravichandran, V., Kashaw, S.K. and Agrawal, R.K., 2012. Recent developments and biological activities of thiazolidinone derivatives: a review. *Bioorg. Med. Chem.*, 20, 3378-3395.

[22] Havrylyuk, D., Mosula, L., Zimenkovsky, B., Vasylenko, O., Gzella, A. and Lesyk, R., 2010. Synthesis and anticancer activity evaluation of 4-thiazolidinones containing benzothiazole moiety. *Eur. J. Med. Chem.*, 45, 5012-5021.

[23] Wang, S., Zhao, Y., Zhang, G., Lv, Y., Zhang, N. and Gong, P., 2011. Design, synthesis and biological evaluation of novel 4-thiazolidinones containing indolin-2-one moiety as potential antitumor agent. *Eur. J. Med. Chem.*, 46, 3509-3518.

[24] Romagnoli, R., Baraldi, P.G., Salvador, M.K., Camacho, M.E., Balzarini, J., Bermejo, J. and Estévez, F., 2013. Anticancer activity of novel hybrid molecules containing 5-benzylidene thiazolidine-2, 4-dione. *Eur. J. Med. Chem.*, 63, 544-557.

[25] Havrylyuk, D., Zimenkovsky, B., Vasylenko, O., Day, C.W., Smee, D.F., Grellier, P. and Lesyk, R., 2013. Synthesis and biological activity evaluation of 5-pyrazoline substituted 4-thiazolidinones. *Eur. J. Med. Chem.*, 66, 228-237.

[26] Havrylyuk, D., Zimenkovsky, B., Vasylenko, O., Gzella, A. and Lesyk, R., 2012. Synthesis of new 4-thiazolidinone-, pyrazoline-, and isatin-based conjugates with promising antitumor activity. *J. Med. Chem.*, 55, 8630-8641.

[27] Wu, J., Yu, L., Yang, F., Li, J., Wang, P., Zhou, W., Qin, L., Li, Y., Luo, J., Yi, Z. and Liu, M., 2014. Optimization of 2-(3-(arylalkyl amino carbonyl) phenyl)-3-(2-methoxyphenyl)-4-thiazolidinone derivatives as potent antitumor growth and metastasis agents. *Eur. J. Med. Chem.*, 80, 340-351.

[28] Kumar, K.S.S., Hanumappa, A., Vetrivel, M., Hegde, M., Girish, Y.R., Byregowda, T.R., Rao, S., Raghavan, S.C. and Rangappa, K.S., 2015. Antiproliferative and tumor inhibitory studies of 2, 3 disubstituted 4-thiazolidinone derivatives. *Bioorg. Med. Chem. Lett.*, 25, 3616-3620.

[29] Senkiv, J., Finiuk, N., Kaminskyy, D., Havrylyuk, D., Wojtyra, M., Kril, I., Gzella, A., Stoika, R. and Lesyk, R., 2016. 5-Ene-4-thiazolidinones induce apoptosis in mammalian leukemia cells. *Eur. J. Med. Chem.*, 117, 33-46.

[30] Appalanaidu, K., Kotcherlakota, R., Dadmal, T.L., Bollu, V.S., Kumbhare, R.M. and Patra, C.R., 2016. Synthesis and biological evaluation of novel 2-imino-4-thiazolidinone derivatives as potent anti-cancer agents. *Bioorg. Med. Chem. Lett.*, 26, 5361-5368.

[31] Cutshall, N.S., O'Day, C. and Prezhdo, M., 2005. Rhodanine derivatives as inhibitors of JSP-1. *Bioorg. Med. Chem. Lett.*, 15, 3374-3379.

[32] Ahn, J.H., Kim, S.J., Park, W.S., Cho, S.Y., Du Ha, J., Kim, S.S., Kang, S.K., Jeong, D.G., Jung, S.K., Lee, S.H. and Kim, H.M., 2006. Synthesis and biological evaluation of rhodanine derivatives as PRL-3 inhibitors. *Bioorg. Med. Chem. Lett.*, 16, 2996-2999.

[33] Park, H., Jung, S.K., Jeong, D.G., Ryu, S.E. and Kim, S.J., 2008. Discovery of novel PRL-3 inhibitors based on the structure-based virtual screening. *Bioorg. Med. Chem. Lett.*, 18, 2250-2255.

[34] Geronikaki, A., Eleftheriou, P., Vicini, P., Alam, I., Dixit, A. and Saxena, A.K., 2008. 2-Thiazolylimino/heteroarylimino-5-arylidene-4-thiazolidinones as new agents with SHP-2 inhibitory action. *J. Med. Chem.*, 51, 5221-5228.

[35] Carter, P.H., Scherle, P.A., Muckelbauer, J.A., Voss, M.E., Liu, R.Q., Thompson, L.A., Tebben, A.J., Solomon, K.A., Lo, Y.C., Li, Z. and Strzemienski, P., 2001. Photochemically enhanced binding of small molecules to the tumor necrosis factor receptor-1 inhibits the binding of TNF-α. *Proc. Natl. Acad. Sci.*, 98, 11879-11884.

[36] Degterev, A., Lugovskoy, A., Cardone, M., Mulley, B., Wagner, G., Mitchison, T. and Yuan, J., 2001. Identification of small-molecule inhibitors of interaction between the BH3 domain and Bcl-xL. *Nat. Cell Biol.*, 3, 173-182.

[37] Dayam, R., Aiello, F., Deng, J., Wu, Y., Garofalo, A., Chen, X. and Neamati, N., 2006. Discovery of small molecule integrin αvβ3 antagonists as novel anticancer agents. *J. Med. Chem.*, 49, 4526-4534.

[38] Jemmezi, F., Kether, F.B.H., Amri, I., Bassem, J. and eddine Khiari, J., Synthesis and biological activity of novel benzothiazole pyridine derivatives. *IOSR JAC.*, 7, 62-66.

[39] Nepali, K., Sharma, S., Sharma, M., Bedi, P.M.S. and Dhar, K.L., 2014. Rational approaches, design strategies, structure activity relationship and mechanistic insights for anticancer hybrids. *Eur. J. Med. Chem.*, 77, 422-487.

[40] Jain, A.K., Vaidya, A., Ravichandran, V., Kashaw, S.K. and Agrawal, R.K., 2012. Recent developments and biological activities of thiazolidinone derivatives: A review. *Bioorg. Med. Chem.*, 20, 3378-3395.

[41] El Ella, D.A.A., Ghorab, M.M., Heiba, H.I. and Soliman, A.M., 2012. Synthesis of some new thiazolopyrane and thiazolopyranopyrimidine derivatives bearing a sulfonamide moiety for evaluation as anticancer and radiosensitizing agents. *Med. Chem. Res.*, 21, 2395–2407.

[42] Eldehna, W.M., Abo-Ashour, M.F., Nocentini, A., Gratteri, P., Eissa, I.H., Fares, M., Ismael, O.E., Ghabbour, H.A., Elaasser, M.M., Abdel-Aziz, H.A. and Supuran, C.T., 2017. Novel 4/3-((4-oxo-5-(2-oxoindolin-3-ylidene) thiazolidin-2-ylidene) amino) benzenesulfonamides: Synthesis, carbonic anhydrase inhibitory activity, anticancer activity and molecular modelling studies. *Eur. J. Med. Chem.*, 139, 250-262.

[43] Narges, K., Tafreshi, Mark C., Lloyd, Marilyn M., Bui, Robert J., Gillies, and David L. Morse, 2014. Carbonic Anhydrase IX as an Imaging and Therapeutic Target for Tumors and Metastases Subcell. *Biochem.* 75, 221–254.

[44] Sedlakova, O., Svastova, E., Takacova, M., Kopacek, J., Pastorek, J. and Pastorekova, S., 2013. Carbonic anhydrase IX, a hypoxia-induced catalytic component of the pH regulating machinery in tumors. *Front Physiol*, 4, 400-414.

[45] Kato, Y., Ozawa, S., Miyamoto, C., Maehata, Y., Suzuki, A., Maeda, T. and Baba, Y., 2013. Acidic extracellular microenvironment and cancer. *Cancer Cell Int.*, 13, 89-96.

[46] Patard, J., Fergelot, P., Karakiewicz, P.I., Klatte, T., Trinh, Q.D. and Rioux-Leclercq, N., 2008. CAIX and VHL status define two types of clear cell renal cell carcinoma: low CAIX expression and absence of VHL gene mutation are associated with tumour aggressiveness and poor survival. *Int. J. Cancer*, 123, 395-400.

[47] Côrte-Real, L., Robalo, M.P., Marques, F., Nogueira, G., Avecilla, F., Silva, T.J., Santos, F.C., Tomaz, A.I., Garcia, M.H. and Valente, A., 2015. The key role of coligands in novel ruthenium (II)-cyclopentadienyl bipyridine derivatives: ranging from non-cytotoxic to highly cytotoxic compounds. *J. Inorg. Biochem*. 150, 148-159.

[48] Akkurt, M., Çelik, Í., Demir, H., Özkırımlı, S. and Büyükgüngör, O., 2011. N-[2-(4-Bromophenyl)-5-methyl-4-oxo-1, 3-thiazolidin-3-yl] pyridine-3-carboxamide. *Acta Crystallogr. Sect. E*, 67,o914-o915.

[49] Syarifah, M.S., Nurhanan, M.Y., Haffiz, J.M., Ilham, A.M., Getha, K., Asiah, O., Norhayati, I., Sahira, H.L. and Suryani, S.A., 2011. Potential anticancer compound from Cerbera odollam. *J. Trop. For. Sci.*, 89-96.

[50] Alexandre, J., Bleuzen, P., Bonneterre, J., Sutherland, W., Misset, J.L., Guastalla, J.P., Viens, P., Faivre, S., Chahine, A., Spielman, M. and Bensmaine, A., 2000. Factors predicting for efficacy and safety of docetaxel in a compassionate-use cohort of 825 heavily pretreated advanced breast cancer patients. *J. Clin. Oncol.*, 18, 562-562.

[51] Badisa, R.B., Ayuk-Takem, L.T., Ikediobi, C.O. and Walker, E.H., 2006. Selective anticancer activity of pure licamichauxiioic-B acid in cultured cell lines. *Pharm. Biol.*, 44, 141-145.

[52] Amresh, P., Kumar, K., Islam, A., Hassan, I. and Ahmad, F., 2013. Receptor chemoprint derived pharmacophore model for development of CAIX inhibitors. *J. Carcinog. Mutagen S, 8*, 17-20.

[53]. Kumari, S., Idrees, D., Mishra, C.B., Prakash, A., Ahmad, F., Hassan, M.I. and Tiwari, M., 2016. Design and synthesis of a novel class of carbonic anhydrase-IX inhibitor 1-(3-(phenyl/4-fluorophenyl)-7-imino-3H-[1, 2, 3] triazolo [4, 5d] pyrimidin 6 (7H) yl) urea. *J. Mol. Graph. Model.*, 64, 101-109.

[54]. Fuhrmann, J., Rurainski, A., Lenhof, H.P. and Neumann, D., 2010. A new Lamarckian genetic algorithm for flexible ligand□receptor docking. *J. Comput. Chem.*, 31, 1911-1918.

[55] G. M. Sheldrick, *SADABS*, version 2.10, University of Göttingen, Germany, (2004)

[56] G. M. Sheldrick, *SHELX, Acta Crystallogr., Sect. A*, 64 (2008) 112–122.

[57] Mosmann, T., 1983. Rapid colorimetric assay for cellular growth and survival: application to proliferation and cytotoxicity assays. *J. Immunol. Methods*, 65(1-2), 55-63.

[58] Alterio, V., Hilvo, M., Di Fiore, A., Supuran, C.T., Pan, P., Parkkila, S., Scaloni, A., Pastorek, J., Pastorekova, S., Pedone, C. and Scozzafava, A., 2009. Crystal structure of the catalytic domain of the tumor-associated human carbonic anhydrase IX. *Proc. Natl Acad. Sci.*, 106, 16233-16238.

[59] Ahmad, K., Roouf Bhat, A., and Athar, F., 2017. Pharmacokinetic Evaluation of Callistemon viminalis Derived Natural Compounds as Targeted Inhibitors Against δ-Opioid Receptor and Farnesyl Transferase. *Lett. Drug Des. Discov.*, 14, 488-499.

[60] Morris, G.M., Goodsell, D.S., Halliday, R.S., Huey, R., Hart, W.E., Belew, R.K. and Olson, A.J., 1998. Automated docking using a Lamarckian genetic algorithm and an empirical binding free energy function. *J. Comput. Chem.*, 19,1639-1662.

[61] Ansari, M.F., Siddiqui, S.M., Ahmad, K., Avecilla, F., Dharavath, S., Gourinath, S. and Azam, A., 2016. Synthesis, antiamoebic and molecular docking studies of furan-thiazolidinone hybrids. *Eur. J. Med. Chem.*, 124, 393-406.

[62] Zaidi, S.L., Agarwal, S.M., Chavalitshewinkoon-Petmitr, P., Suksangpleng, T., Ahmad, K., Avecilla, F. and Azam, A., 2016. Thienopyrimidine sulphonamide hybrids: design, synthesis, antiprotozoal activity and molecular docking studies. *RSC Adv.*, 6, 90371-90383.

Caption

Figure 1: Structure of some Thiazolidinone based drugs which are currently used for the treatment of various disease.

Figure 2: Structure of some thiazolidinone derivatives showing anticancer activity.

Figure 3: ORTEP plot for the compound of 2(Phenylimino)-3-(pyridine-4-ylmethyl) thiazolidin-4-one (**2**). All the non-hydrogen atoms are presented by their 50% probability ellipsoids. Hydrogen atoms are omitted for clarity.

Figure 4: ORTEP plot for the compound of 5-Benzylidene-2-phenylimino-3-pyridine-4-ylmethyl-thiazolidin-4-one (**3**). All the non-hydrogen atoms are presented by their 50% probability ellipsoids. Hydrogen atoms are omitted for clarity.

Figure 5: ORTEP plot for the compound of 5-(4-Methoxybenzylidene)-2-(phenylimino)-3-(pyridine-4-ylmethyl)thiazolidin-4-one (**6**). All the non-hygrogen atoms are presented by their 50% probability ellipsoids. Hydrogen atoms are omitted for clarity.

Figure 6: ORTEP plot for the compound of -(3,4-Dimethoxy-benzylidene)-2-(phenylimino)-3-(pyridine-4-ylmethyl)thiazolidine-4-one (**12**). All the non-hygrogen atoms are presented by their 50% probability ellipsoids. Hydrogen atoms are omitted for clarity.

Figure 7: Enantiomers present in the compound 2(Phenylimino)-3-(pyridine-4-ylmethyl) thiazolidin-4-one (**2**). Enantiomerization occurs by simultaneously rotating about the two single bonds, N(1)-C(10) and N(2)-C(4) (**Figure 3**). Drawings were done with mercury 2.3 program with balls and sticks.

Figure 8: Enantiomers present in the compound 5-Benzylidene-2-phenylimino-3-pyridine-4-ylmethyl-thiazolidin-4-one (**3**). Enantiomerization occurs by simultaneously rotating about the two single bonds, N(1)-C(10) and N(2)-C(4) (**Figure 4**). Drawings were done with mercury 2.3 program with balls and sticks.

Figure 9: Enantiomers present in the compound 5-(4-Methoxybenzylidene)-2-(phenylimino)-3-(pyridine-4-ylmethyl)thiazolidin-4-one (**6**). Enantiomerization occurs by simultaneously rotating about the two single bonds, N(1)-C(10) and N(2)-C(4) (**Figure 5**). Drawings were done with mercury 2.3 program with balls and sticks.

Figure 10: Enantiomers present in the compound 5-(3,4-Dimethoxy-benzylidene)-2-(phenylimino)-3-(pyridine-4-ylmethyl)thiazolidine-4-one (**12**). Enantiomerization occurs by simultaneously rotating about the two single bonds, N(1)-C(10) and N(2)-C(4) (**Figure 6**). Drawings were done with mercury 2.3 program with balls and sticks.

Figure 11: View along edge of the crystal packing of compounds, **2**, **3**, **6** and **12**.

Figure 12: Fluorescence binding studies: (A). Fluorescence emission spectra of CAIX titrated with compound **8**, Quenching in fluorescence intensity after the addition of compound indicating binding. **(B).** Modified Stern-Volmer plot (log (Fo-F)/F versus log [L]).

Figure 13: Fluorescence binding studies: (A). Fluorescence spectra of CAIX were titrated with compound **11** gradually adding compounds with increasing concentration, fluorescence intensity was quenched indicating binding. **(B).** Plot between log (Fo-F)/F versus log [L].

Figure 14: Molecular docking studies: (**A, C**) Cartoon view of compound **8** and **11** docked with CAIX. (**B D**,) Shows the active site residues interact with compound **8** and **11**.

Residues of CAIX are shown with ball and stick and compounds are shown with stick model. Hydrogen bonds are shown as broken lines (black).

Tables Legends:

Table 1: Crystal Data and Structure Refinement for 2(Phenylimino)-3-(pyridine-4-ylmethyl)thiazolidin-4-one (**2**), 5-Benzylidene-2-phenylimino-3-pyridine-4-ylmethyl-thiazolidin-4-one (**3**), 5-(4-Methoxybenzylidene)-2-(phenylimino)-3-(pyridine-4-ylmethyl)thiazolidin-4-one (**6**) and 5-(3,4-Dimethoxy-benzylidene)-2-(phenylimino)-3-(pyridine-4-ylmethyl)thiazolidine-4-one (**12**).

Table 2: Cytotoxic activity of the synthesized pyridine-thiazolidinone derivatives against HEK-293, MCF-7 and HepG2 cell lines, selective index, binding affinity on CA IX and fluorescence binding study

Table 3: Binding energy and specific interaction of CA IX with compound

Scheme:

Scheme 1: Synthesis of pyridine-thiazolidinone derivatives (**3-20**)

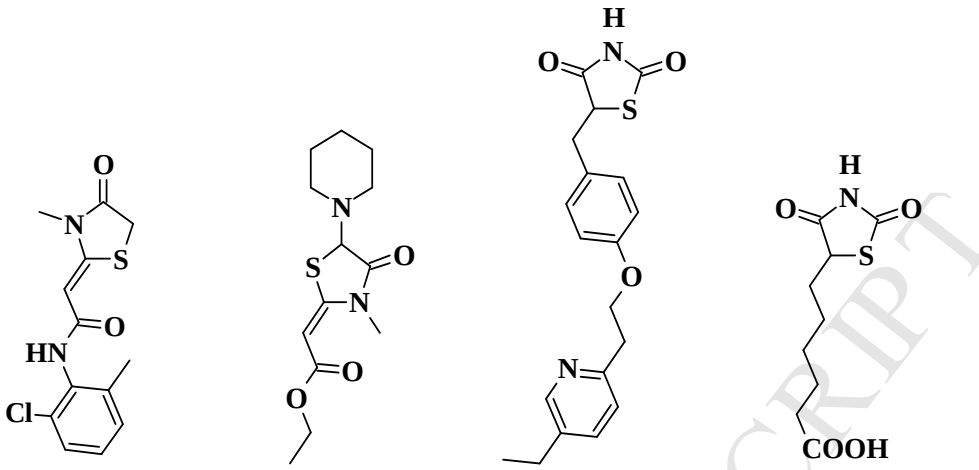

Figure 1: Structure of some Thiazolidinone based drugs which are currently used for the treatment of various disease.

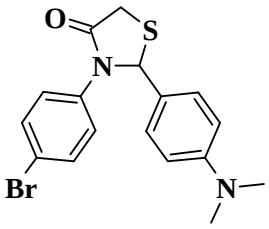

IC_{50} = 11.9 µM (Reh)

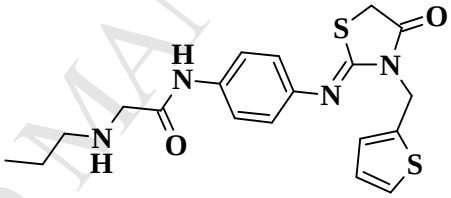

IC_{50} = 3.4 ± 2 µM (B16F10)

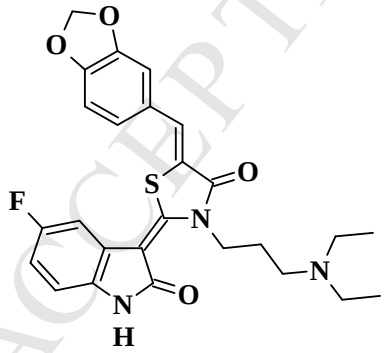

IC_{50} = 0.025 ± 0.008 (HT-29)

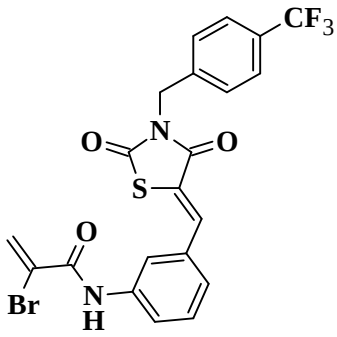

IC_{50} = 0.72 ± 0.04 (L1210)

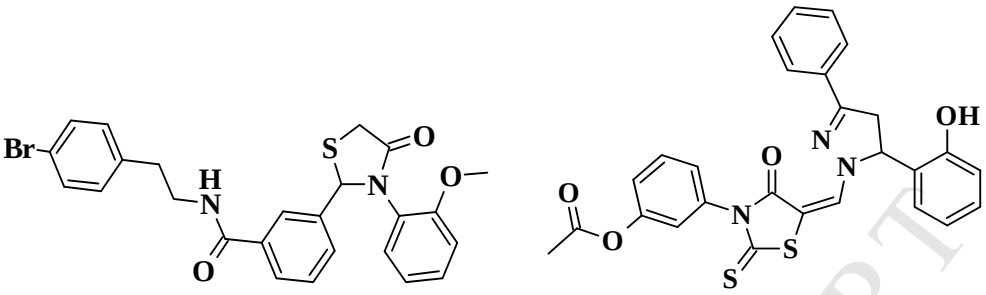

IC_{50} = 0.21 (A549) IC_{50} = 0.118 ± 0.009 (HL-60)

Figure 2: Structure of some thiazolidinone derivatives showing anticancer activity.

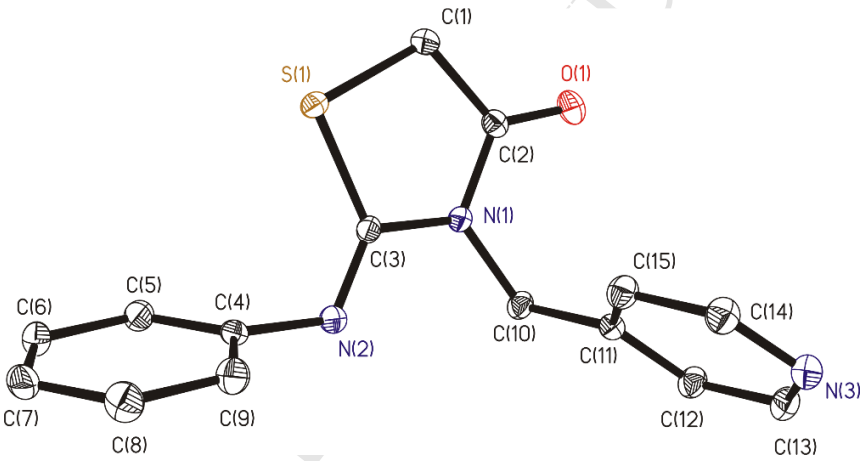

Figure 3: ORTEP plot for the compound of 2(Phenylimino)-3-(pyridine-4-ylmethyl)thiazolidin-4-one (**2**). All the non-hygrogen atoms are presented by their 50% probability ellipsoids. Hydrogen atoms are omitted for clarity.

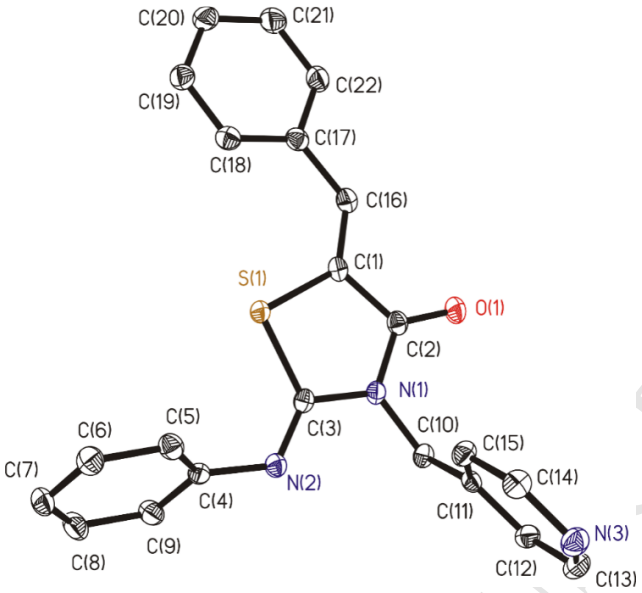

Figure 4: ORTEP plot for the compound of 5-Benzylidene-2-phenylimino-3-pyridine-4-ylmethyl-thiazolidin-4-one (**3**). All the non-hydrogen atoms are presented by their 50% probability ellipsoids. Hydrogen atoms are omitted for clarity.

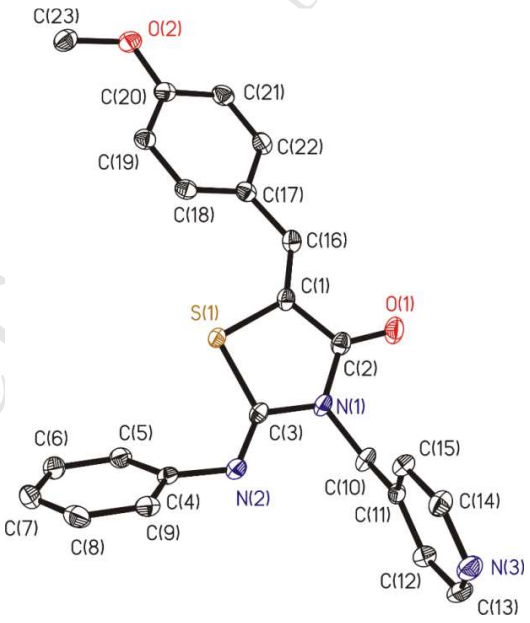

Figure 5: ORTEP plot for the compound of 5-(4-Methoxybenzylidene)-2-(phenylimino)-3-(pyridine-4-ylmethyl)thiazolidin-4-one (**6**). All the non-hygrogen atoms are presented by their 50% probability ellipsoids. Hydrogen atoms are omitted for clarity.

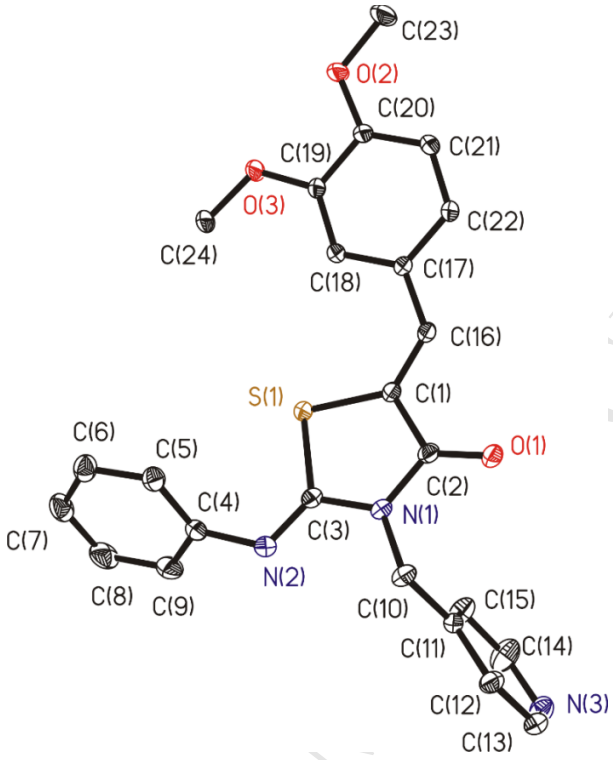

Figure 6: ORTEP plot for the compound of (3,4-Dimethoxy-benzylidene)-2-(phenylimino)-3-(pyridine-4-ylmethyl)thiazolidine-4-one (**12**). All the non-hygrogen atoms are presented by their 50% probability ellipsoids. Hydrogen atoms are omitted for clarity.

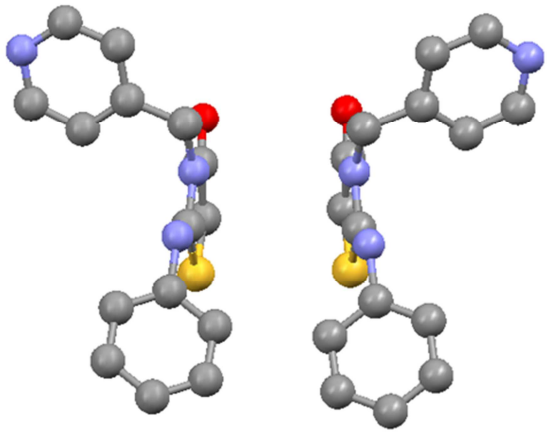

Figure 7: Enantiomers present in the compound 2(Phenylimino)-3-(pyridine-4-ylmethyl) thiazolidin-4-one (**2**). Enantiomerization occurs by simultaneously rotating about the two single

bonds, N(1)-C(10) and N(2)-C(4) (**Figure 3**). Drawings were done with mercury 2.3 program with balls and sticks.

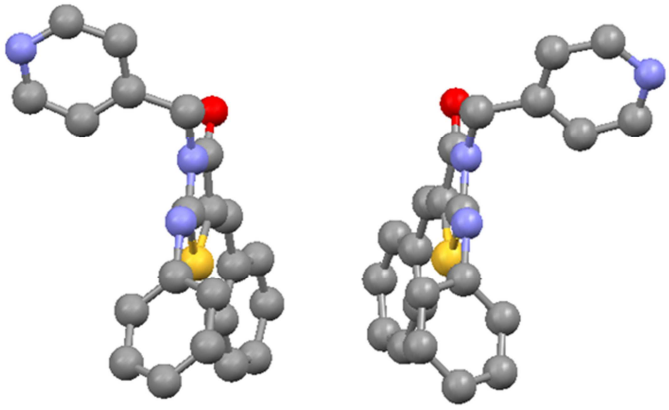

Figure 8: Enantiomers present in the compound 5-Benzylidene-2-phenylimino-3-pyridine-4-ylmethyl-thiazolidin-4-one **(3)**. Enantiomerization occurs by simultaneously rotating about the two single bonds, N(1)-C(10) and N(2)-C(4) **(Figure 4).** Drawings were done with mercury 2.3 program with balls and sticks.

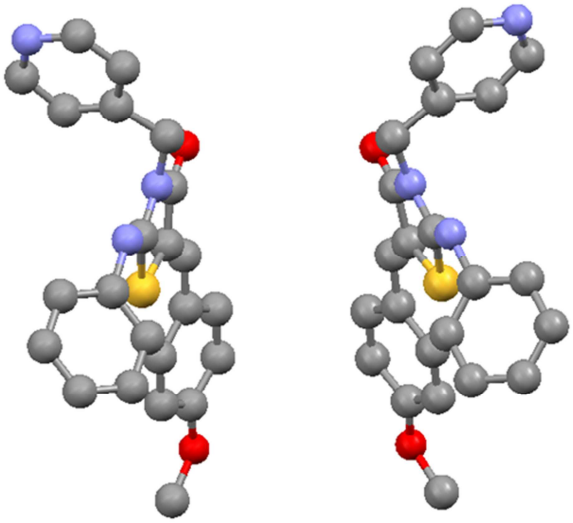

Figure 9: Enantiomers present in the compound 5-(4-Methoxybenzylidene)-2-(phenylimino)-3-(pyridine-4-ylmethyl)thiazolidin-4-one **(6)**. Enantiomerization occurs by simultaneously rotating about the two single bonds, N(1)-C(10) and N(2)-C(4) **(Figure 5)**. Drawings were done with mercury 2.3 program with balls and sticks.

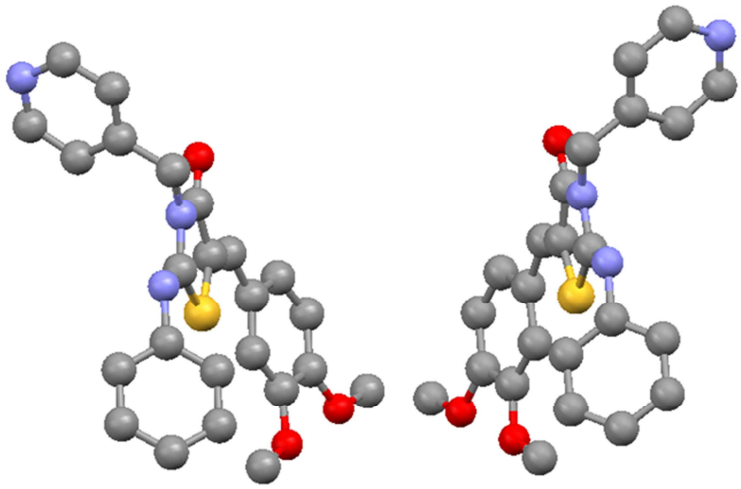

Figure 10: Enantiomers present in the compound 5-(3,4-Dimethoxy-benzylidene)-2-(phenylimino)-3-(pyridine-4-ylmethyl)thiazolidine-4-one **(12)**. Enantiomerization occurs by simultaneously rotating about the two single bonds, N(1)-C(10) and N(2)-C(4) **(Figure 6).** Drawings were done with mercury 2.3 program with balls and sticks.

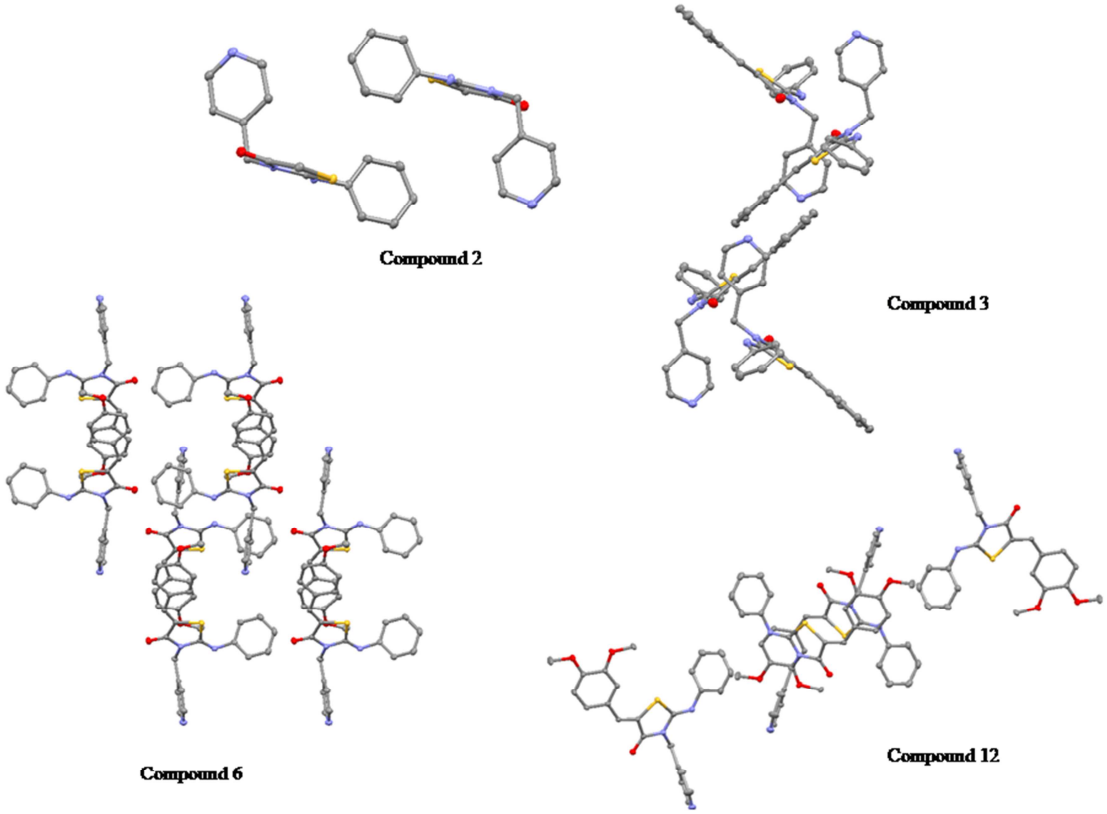

Figure 11: View along edge of the crystal packing of compounds **2**, **3**, **6** and **12**.

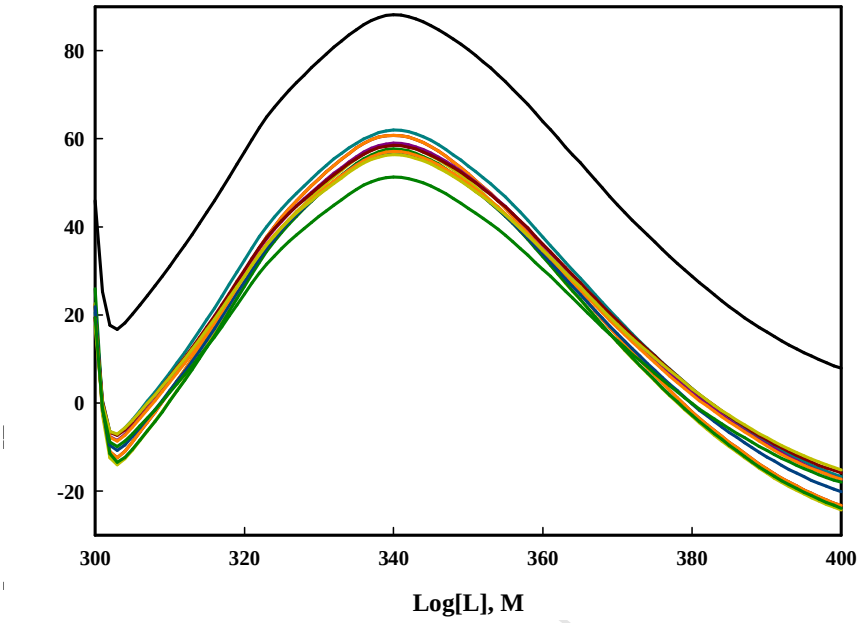

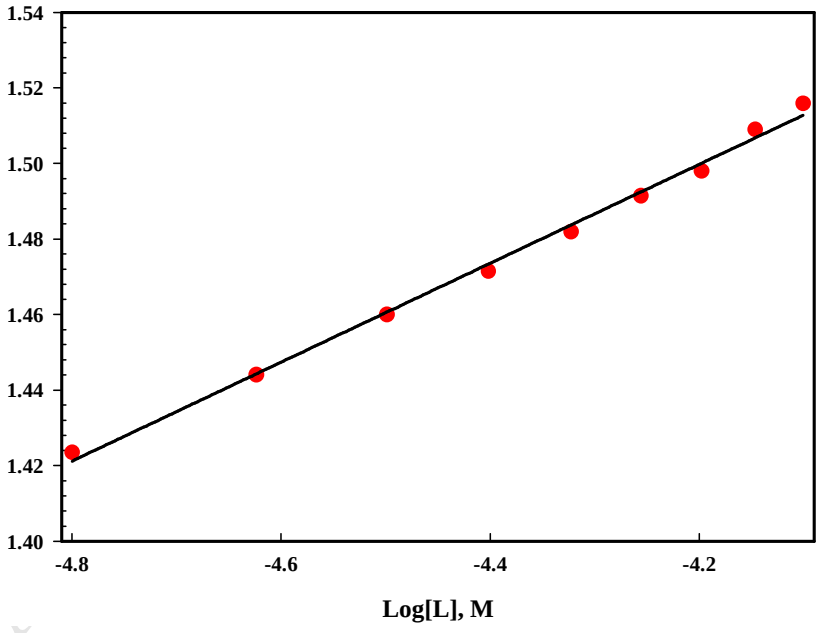

Figure 12: Fluorescence binding studies: (A). Fluorescence emission spectra of CAIX titrated with compound **8**, Quenching in fluorescence intensity after the addition of compound indicating binding. **(B).** Modified Stern-Volmer plot (log (Fo-F)/F versus log [L]).

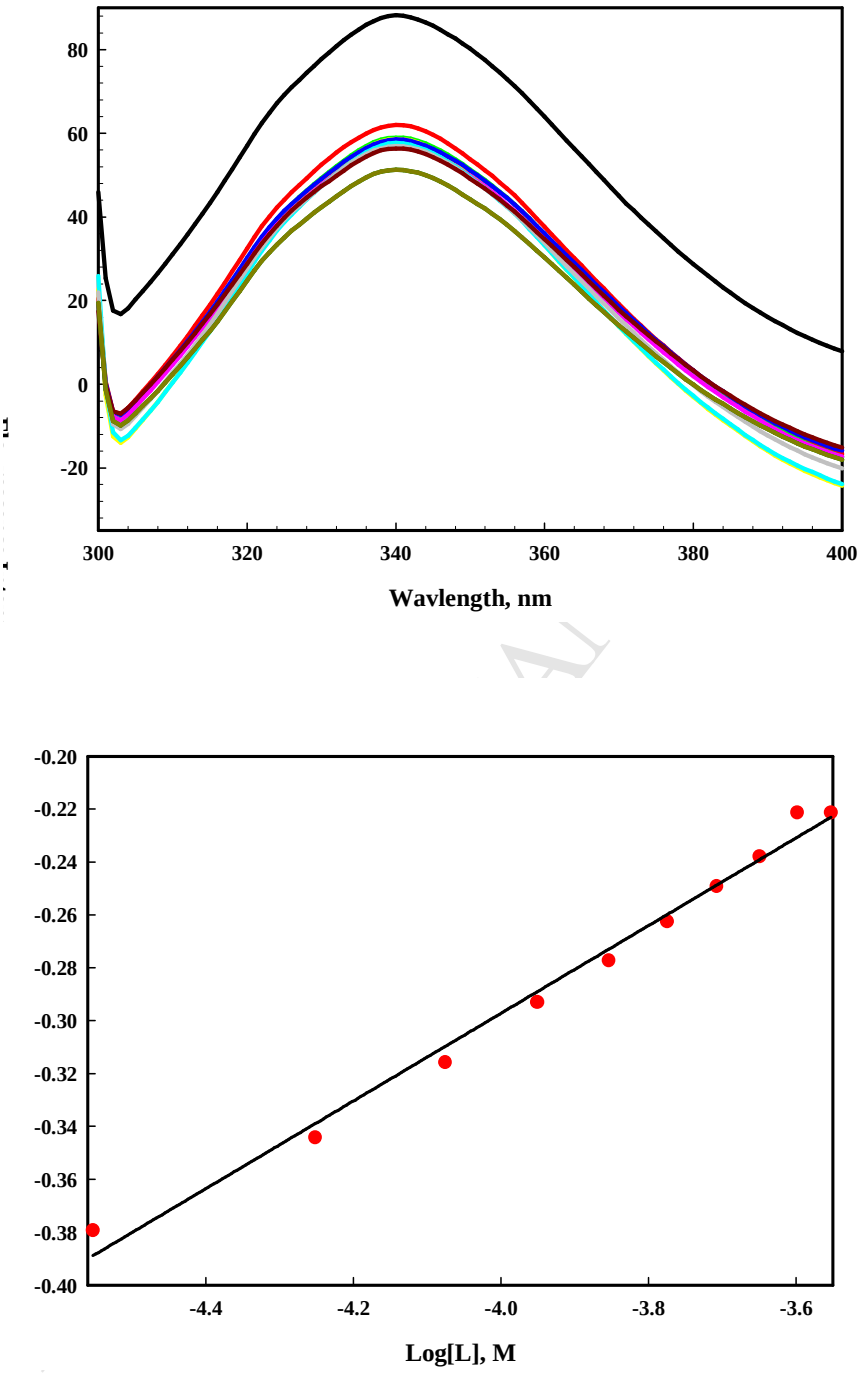

Figure 13: Fluorescence binding studies: (A). Fluorescence spectra of CAIX were titrated with compound **11** gradually adding compounds with increasing concentration, fluorescence intensity was quenched indicating binding. **(B).** Plot between log (Fo-F)/F versus log [L].

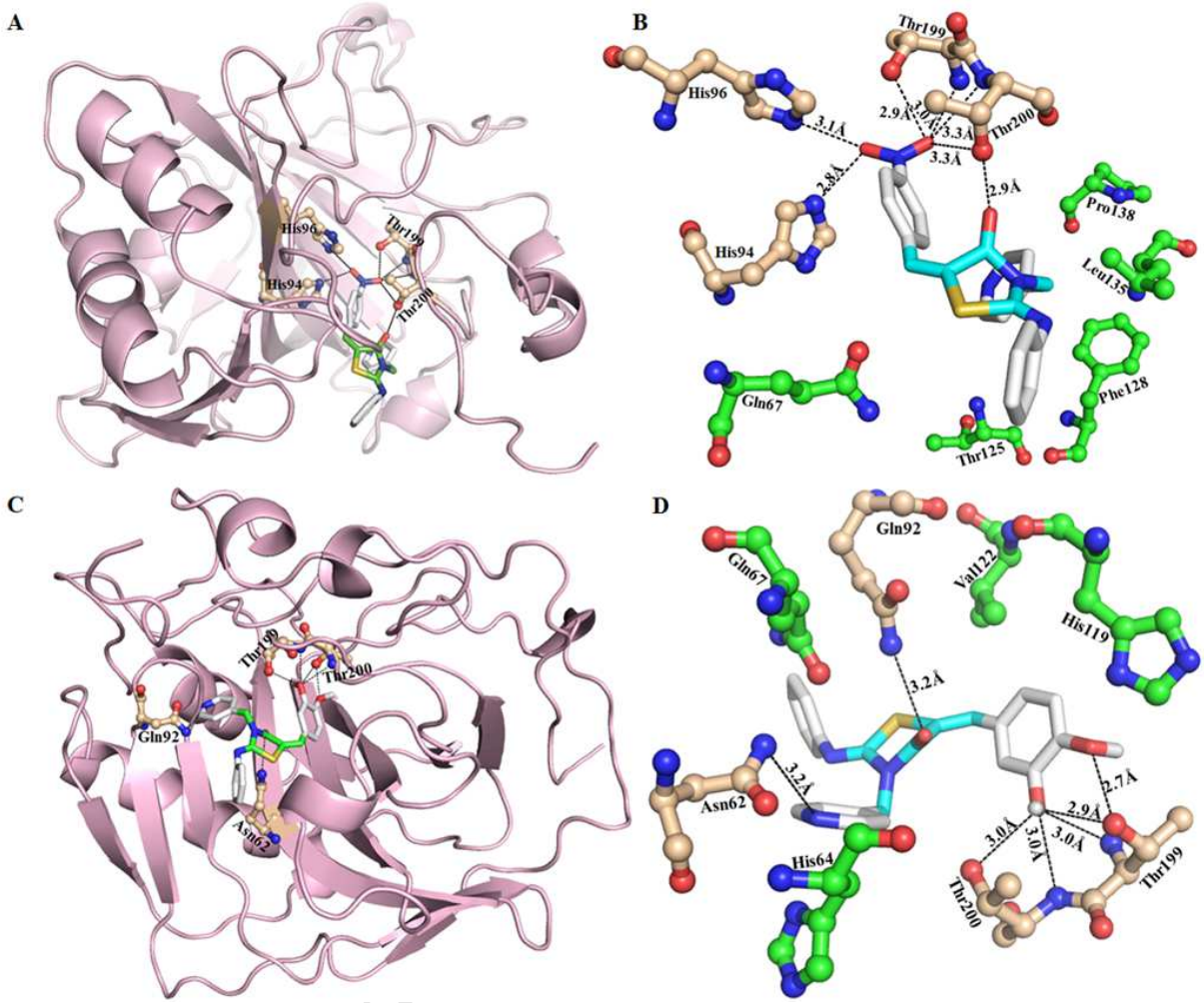

Figure 14: Molecular docking studies: (**A, C**) Cartoon view of compound **8** and **11** docked with CAIX. (**B D**,) Shows the active site residues interact with compound **8** and **11**. Residues of CAIX are shown with ball and stick and compounds are shown with stick model. Hydrogen bonds are shown as broken lines (black).

Table 1: Crystal Data and Structure Refinement for 2(Phenylimino)-3-(pyridine-4-ylmethyl)thiazolidin-4-one (**2**), 5-Benzylidene-2-phenylimino-3-pyridine-4-ylmethyl-thiazolidin-4-one (**3**), 5-(4-Methoxybenzylidene)-2-(phenylimino)-3-(pyridine-4-ylmethyl)thiazolidin-4-one (**6**) and 5-(3,4-Dimethoxy-benzylidene)-2-(phenylimino)-3-(pyridine-4-ylmethyl)thiazolidine-4-one (**12**).

	2	**3**	**6**	**12**
Formula	$C_{15}H_{13}N_3OS$	$C_{22}H_{17}N_3OS$	$C_{23}H_{19}N_3O_2S$	$C_{24}H_{21}N_3O_3S$
Formula weight	283.34	371.45	401.47	431.50
T, *K*	100(2)	105(2)	98(2)	99(2)
Wavelength, Å	0.71073	0.71073	0.71073	0.71073
Crystal system	Triclinic	Monoclinic	Monoclinic	Monoclinic
Space group	$P\bar{1}$	$P2_1/n$	C2/c	$P2_1/n$
a/Å	6.9485(2)	14.7764(4)	9.8941(3)	9.0174(4)
b/Å	10.2150(2)	5.77200(10)	19.4864(5)	23.7708(9)
c/Å	10.8745(3)	21.4727(5)	20.3057(5)	10.5727(4)
α/º	63.1787(10)	90	90	90
β/º	78.7277(12)	96.5905(10)	95.5604(14)	111.4377(18)
γ/º	76.3612(11)	90	90	90
V/Å^3	665.86(3)	1819.29(7)	3896.53(18)	2109.48(15)
Z	2	4	8	4
F_{000}	296	776	1680	904
D_{calc}/g cm^{-3}	1.413	1.356	1.369	1.359
μ/mm^{-1}	0.241	0.195	0.191	0.185
θ/ (º)	2.11 to 30.54	1.59 to 29.50	2.02 to 28.36	1.71 to 30.14
R_{int}	0.0200	0.0263	0.0327	0.0278

Crystal size/ mm^3	0.48 x 0.47 x 0.45	0.45 x 0.45 x 0.43	0.50 x 0.41 x 0.34	0.48 x 0.38 x 0.37
Goodness-of-fit on F^2	1.095	1.054	1.073	1.109
$R_1[I>2\sigma(I)]$ [a]	0.0305	0.0325	0.0320	0.0344
wR_2 (all data) [b]	0.0844	0.0870	0.0959	0.1105
Largest differences peak and hole ($eÅ^{-3}$)	0.503 and -0.205	0.346 and -0.293	0.344 and -0.279	0.469 and -0.425

[a] $R_1 = \Sigma||F_o|-|F_c||/\Sigma|F_o|$. [b] $wR_2 = \{\Sigma[w(||F_o|^2-|F_c|^2|)^2]|/\Sigma[w(F_o^2)^2]\}^{1/2}$

Table 2: Cytotoxic activity of the synthesized pyridine-thiazolidinone derivatives against HEK-293, MCF-7 and HepG2 cell lines, selective index, binding affinity on CA IX and fluorescence binding study

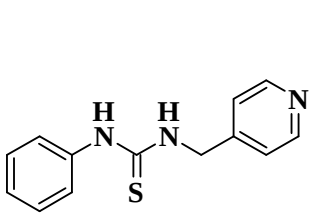

1

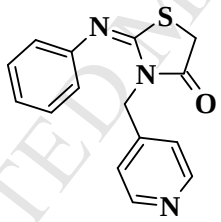

2

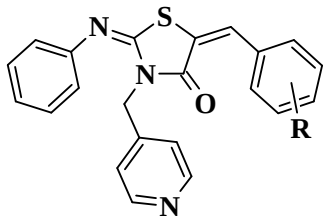

3-20

Compound No.	Ar-R	Esterase assay IC50 (µM)		Fluorescence binding study IC_{50} (µM)	HEK-293	MCF-7		HepG-2	
		CAIX	CAII						
1	-	17.95	N.D	N.D	47.2±1.41	37.3±1.41	1.2	19.3±1.41	2.4

2	-	26.15	N.D	N.D	99.5±2.82	65.8±1.35	1.5	26.0±2.47	**3.8**
3	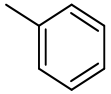	50.92	N.D	N.D	64.7±1.27	26.4±2.26	2.4	25.16±3.67	2.5
4	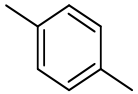	57.31	N.D	N.D	49.47±0.42	36.9±0.79	1.3	19.7±1.69	2.5
5	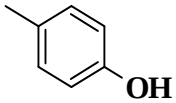	6.72	N.D	N.D	142.3±2.19	18.9±2.19	**7.5**	11.8±1.95	**12.0**
6	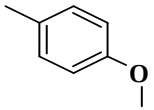	40.41	N.D	N.D	47.9±0.35	31.5±1.34	1.5	19.1±2.47	2.5
7	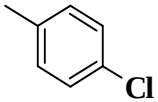	40.18	N.D	N.D	42.3±0.63	54.9±2.07	1.1	28.8±1.48	1.4
8	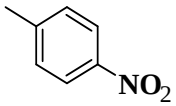	1.61	14.44	11.21	249.6±0.83	13.0±2.28	**19.2**	18.9±1.34	**13.2**

9	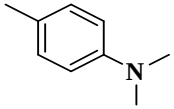	32.89	N.D	N.D	122.4±0.74	76.3±1.56	1.6	52.6±1.45	2.3
10	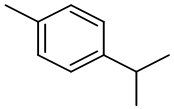	63.11	N.D	N.D	137.2±0.63	53.3±2.05	2.5	32.3±1.48	**4.2**
11	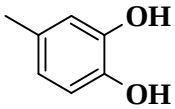	1.84	27.18	2.32	230.4±0.72	12.4±1.39	**18.5**	16.2±1.34	**14.2**
12	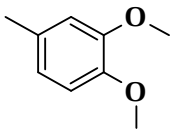	20.92	N.D	N.D	171.4±0.86	80.7±1.96	2.1	28.9±1.13	**5.9**
13	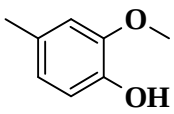	60.92	N.D	N.D	67.4±0.77	28.0±2.05	2.4	28.6±1.15	2.3
14	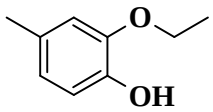	38.40	N.D	N.D	46.5±1.06	20.1±1.06	2.3	20.4±1.06	2.2
15	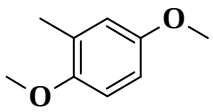	16.68	N.D	N.D	80.1±0.66	37.0±1.45	2.1	35.8±1.45	2.2

16	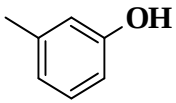	10.81	N.D	N.D	149.6±1.04	43.6±1.13	**3.4**	17.6±2.12	**8.5**
17	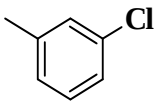	43.52	N.D	N.D	71.8±1.13	29.8±1.69	2.4	28.9±2.40	2.4
18	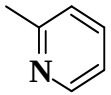	6.64	N.D	N.D	161.3±2.33	21.1±2.68	**7.6**	31.0±1.90	**5.2**
19	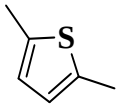	10.04	N.D	N.D	146.4±1.54	28.7±1.90	**5.1**	23.1±1.90	**6.3**
20	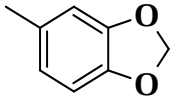	58.39	N.D	N.D	64.8±0.84	35.2±1.93	1.8	24.4±2.68	2.6
21	Doxorubicin	N.D	N.D	N.D	148.4±1.99	18.5±1.59	**8.0**	21.2±1.27	**7.0**
22	AZM	0.0709	N.D	N.D	N.D	N.D	N.D	N.D	N.D

IC_{50} (µM) and selectivity index (SI) values of Compounds on HEK-293, MCF-7 and HepG-2 cell lines.

Table 3: Binding energy and specific interaction of CA IX with compounds **8, 11** and AZM

Compound	Binding energy(kcal/mol)	Inhibitory constant(μM)	Protein ligands interaction		
			No. of H bonds	Amino acid residues	Distance (Å)
8	−8.95	7.01	7	His94 His96 Thr199 Thr200	2.8 3.1 2.9, 3.0, 3.3 2.9, 3.3
11	-8.01	10.21	7	Asn62 Gln92 Thr199 Thr200	3.2 3.2 2.7, 2.9, 3.0 3.0, 3.0
AZM	-6.43	14.04	9	His64 Gln67 His94 His96 Thr199 Thr200	1.6 1.9 1.9 3.1 2.9, 2.9, 3.2 2.9, 2.9

Scheme 1: Synthesis of pyridine-thiazolidinone derivatives (3-20)

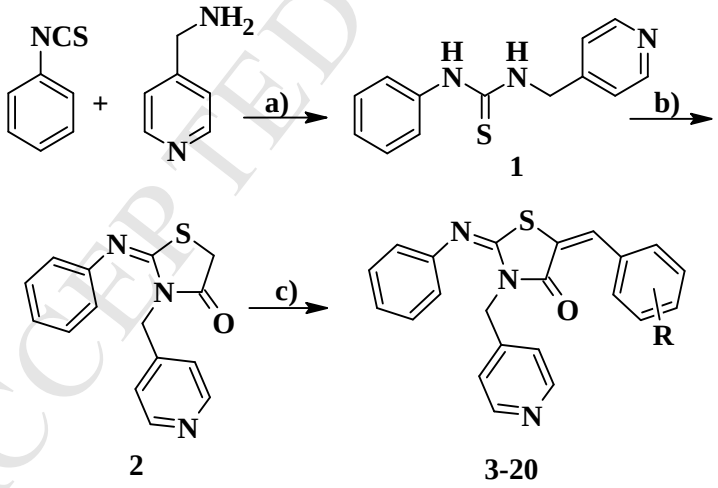

Reagents and conditions: *(a) Toluene, r.t., 1 h. (b) sodium acetate, chloroacetic acid, ethanol, reflux, 14 h. (c) different aldehyde, piperidine, ethanol, reflux, 12-14 h.*

Research Highlights

- Pyridine-thiazolidinone derivatives were synthesized.
- Compounds were evaluated for anticancer activity on MCF-7 and HepG2 cell lines.
- Cytotoxicity of compounds were performed on HEK cell line.
- Two compounds showed most promising anticancer activity and significant inhibition on CAIX.
- Molecular docking study was performed on CAIX.